Non-Common Path Error in the Palomar 200-inch Adaptive Optics System

Joseph C. Carson and Lilit Abramyan[1]
Jet Propulsion Laboratory, Earth & Space Sciences, 4800 Oak Grove Dr., Pasadena, CA 91109

October 7, 2006

Abstract

The Palomar Hale Telescope Adaptive Optics (AO) system uses active adjustment of the telescope light path to correct for atmospheric distortion and achieve diffraction-limited images. Located at the cassegrain focus of the telescope, the AO system and science camera experience a gravitational force whose direction changes according to telescope position. As this gravitational vector varies with telescope pointing, the AO optical bench, the optical mounts, and the optical components may flex, resulting in image motion on the detector. The AO system wavefront sensor partly monitors this flexure, and corrects for it. Flexure that occurs downstream of this sensor though will persist and create an image motion on the detector. To quantify this effect, we observed an AO internal calibration source, while we moved the telescope along constant declinations. From this data, we were able to reduce a single equation, for each x and y dimension, that describes detector image motion as a function of telescope position.

As an additional test, we also collected image drift data using a visible camera that intercepted the visible portion of the light path just upstream of the PHARO (Palomar High Angular Resolution Observer) science camera. An analysis of the data revealed that the visible camera observed image drift that matched the PHARO science camera drift to within ~15%. This fact suggests that the main source of the image drift is occurring upstream of the visible camera location, and not inside the PHARO science camera or at the entrance window interface. It also suggests that a system that collects image drift data at the visible camera location, and actively returns feedback to the AO system, could, in principle, reduce PHARO image drift by ~85%.

Introduction

When light from a star or other astronomical source enters the earth's atmosphere, turbulence distorts the incoming wavefront, causing a blurring to result when that object is imaged by a telescope detector. This blurring prevents a telescope from resolving images at the telescope's fundamental diffraction limit. The Palomar Hale Telescope employs an adaptive optics system (Troy et al., 2000) that uses a wavefront sensor to monitor the distorting effects of atmospheric distortion on an observed guide star. The system then sends commands, at a rate of several thousand times a second, to a tip/tilt and deformable mirror, which adjust the optical path to remove the distorting effect. As a result, the downstream PHARO near-Infrared science camera (Hayward et al. 2001) is able to resolve sources at the telescope's diffraction limit. Such a phenomenon translates to the telescope system being able to achieve a resolution, at near-IR wavelengths, that is superior to space-based observatories such as the Hubble Space Telescope.

Generating a diffraction-limited stellar point spread function (PSF) on the detector requires that the telescope system must be able to keep the source precisely located at a given detector position. If the source position drifts over the course of the exposure, a blurring may occur. Figure 1 represents image blurring that results from a 4.2-pixel (106-arcsecond) drift in target pointing. Even if the telescope points perfectly accurately, target drift may occur as a result of internal flexure within the AO system and PHARO science camera. Since this system is located at the

1 Current Address: Glendale Community College, Glendale, CA 91208

cassegrain focus of the Palomar Telescope, such flexure is encouraged by the changing direction of the gravity vector. The wavefront-sensor/dichroic unit may observe this effect and therefore help correct it by adjusting the optical path. However, flexure occurring downstream of the dichroic will persist in a blurring effect. To quantify this effect, we take exposures of an AO internal calibration source as we move the telescope along constant declinations.

In addition to these PHARO camera tests, we collect target drift data with a visible camera located upstream of the PHARO entrance window, but downstream of the wavefront sensor dichroic. Comparing this visible camera data with the PHARO camera data, we are able to gain insights on the location of the flexure source.

Experimental Procedures

On February 16, 2006 observations, we used the Adaptive Optics internal HeNe laser light source as our "guide star". With the PHARO science camera we tracked PSF drift as we pointed the telescope to different positions. With the cassegrain ring angle at -24.00 degrees, we took five 1.416-second exposures at each of five declinations (+3, +18, +33, +48, +63 degrees) and seven hour angles (3, 2, 1, 0, -1, -2, -3 hours). The AO Tip/Tilt mirror was on and the Deformable Mirror was off. The PHARO platescale was set to 25 mas/pixel; the Slit wheel was set to 25 arcsecond field; the Lyot wheel was open, and the Grism wheel was open. We chose to not use any chromatic filters since the near-IR detector (HAWAII) could only detect the HeNe laser light when all the filters were removed. We chose to use the HeNe laser instead of the AO internal white light source because we were simultaneously conducting observations with a visible camera on the AO bench, which was more sensitive to the HeNe laser light.

The visible flexure camera (Prosilica EC750) was positioned just behind the "Fold Mirror" labeled in the lower-right of Figure 2. The labeled "Fold Mirror" had been replaced by a dichroic and is therefore a misnomer in the Figure 2 rendering. This dichroic, while reflecting near-IR light to the PHARO camera, transmitted the visible light that had leaked through the wavefront sensor dichroic. The transmitted visible light was detected by the visible camera, positioned at the light-source focal plane. For our experiment, the Flexure Camera took continuous 1-second exposures. A connected Windows-based control program performed an automated centroid fit to the recorded PSF and wrote the centroid coordinates to file. Through the course of our data collection, we periodically turned the laser light source on and off to ensure that we could accurately sync up flexure camera data points with PHARO camera data points.

Analysis

Using IDL to perform Gaussian fits of the PHARO PSFs, the coordinates of the centers of the source positions were located. We medianed the centroid positions of each five-exposure set to record a single PSF position for each combination of hour angle and declination. In an ideal environment, with no target drift, the position should remain constant over all hour angles and declinations. Because of adverse effects like optical bench flexure, the position varies according to the telescope position. To observe this effect, we plotted PSF X-pixel and Y-pixel positions with respect to hour angle (see Figure 3). For each of the declination curves, we fitted a second order polynomial function in the form: $target\text{-}shift = a + b\ ha + c\ ha^2$; *ha* is the telescope hour angle, measured in degrees east of zenith. *target-shift* is measured in units of arcseconds, as an offset from the target's original measured position (corresponding to a 45-degree hour angle position). .

To generate single equations to predict drift for any combination of declination and hour angle, we first plotted the aforementioned coefficients (*a*, *b*, and *c*) as a function of telescope declination. A function was then fitted to each of the coefficient curves. These functions allowed us to output coefficients for any declination. Combining functions, we generated a single function that described the expected target star position for any combination of declination and hour angle:

$$X\text{-}Shift = [\,1.20 - 0.0186\,d + 0.000125\,d^2\,] + [\,-0.0286 + 0.0000542\,d - 0.000000111\,d^2\,]\,ha + [\,0.0000331 + 0.00000752\,d - 0.0000000487\,d^2\,]\,ha^2 \quad \textbf{(Equation 1)}$$

$$Y\text{-}Shift = [\,0.777 + 0.00816\,d - 0.0000910\,d^2\,] + [\,-0.00957 + 0.0000275\,d + 0.000000217\,d^2\,]\,ha + [\,-0.000166 - 0.00000508\,d - 0.0000000460\,d^2\,]\,ha^2 \quad \textbf{(Equation 2)}$$

d is the declination and *ha* is the telescope's east-west position, measured in degrees east of zenith. *X-Shift* and *Y-Shift* are measured in arcsecond units. They represent the target's displacement from a starting position, corresponding to a 45-degree telescope hour angle. We may take the derivative of the above equations to deduce the rate of drift (arcseconds/hour-angle-degrees) for any combination of declination and hour angle:

$$X\text{-}Shift\text{-}Rate = (\,-0.0286 + 0.0000542\,d - 0.000000111\,d^2\,) + (\,0.0000331 + 0.00000752\,d - 0.0000000487\,d^2\,)\,ha \quad \textbf{(Equation 3)}$$

$$Y\text{-}Shift\text{-}Rate = [\,-0.00957 + 0.0000275\,d + 0.000000217\,d^2\,] + [\,-0.000166 - 0.00000508\,d - 0.0000000460\,d^2\,]\,ha \quad \textbf{(Equation 4)}$$

X-Shift-Rate and *Y-Shift-Rate* are measured in units of arcseconds/hour-angle-degrees.

Figure 3 shows PHARO drift data for five different declinations. Over-plotted are curves derived from equations 1 and 2. The fitted curves differ from the experimental curves by a typical level of 0.22% in X (~0.021 arcseconds) and 0.12% in Y (~0.008 arcseconds).

A comparison of PHARO camera drift with visible camera drift helps reveal information on the source location of target drift. For instance, if visible camera drift has little similarity to PHARO camera drift, that would be a strong indication that the source of such drift, such as optical bench flexure, would be occurring somewhere between the visible camera dichroic and the PHARO detector plane. Conversely, if visible camera and PHARO camera drift closely resemble one another, that suggests that the source of error occurs upstream of the visible camera dichroic. To take advantage of these facts, we plotted together PHARO and visible camera data with respect to hour angle (see Figure 4). We used the laser light on-off instances (see previous section) to properly sync visible camera data points with PHARO camera data points. As observed from Figures 5, the visible camera data tracks the PHARO data drift to within ~15%.

Conclusions

We conducted on-telescope tests and follow-up data analysis to quantify target drift in the Palomar Adaptive Optics System and PHARO science camera (see figures 3 and 4). Polynomial fits to the experimental data set produce a single equation, for each of the detector *x* and *y* dimensions, that describes detector image motion as a function of telescope position (see equations 1 through 4). A comparison of PHARO camera drift with visible camera drift, measured upstream in the optical path, indicated that the two detectors recorded target motion that agreed within about a 15% level. This fact suggests that a dedicated visible camera placed at this location should be able to serve as a useful indicator of target drift. K. Wallace (JPL) has recently installed and begun testing on such a system.

ACKNOWLEDGMENTS
We thank Jeff Hickey, Rick Burruss, and the Palomar staff for their invaluable support of these observations. We thank Kent Wallace for his support of visible camera tests, as well as his general advice and guidance. Lilit Abramyan was supported by the JPL Minority Education Initiatives program. This study is based on experiments performed at the Hale Telescope, Palomar Observatory, as part of a continuing collaboration between the California Institute of Technology, NASA/JPL, and Cornell University. The data analysis was carried out at the Jet Propulsion Laboratory, California Institute of Technology, under a contract with the National Aeronautics and Space Administration.

References
Hayward et al. 2001, *PASP*, 113, 105
Troy et al., 2000, *SPIE*, 4007, 31

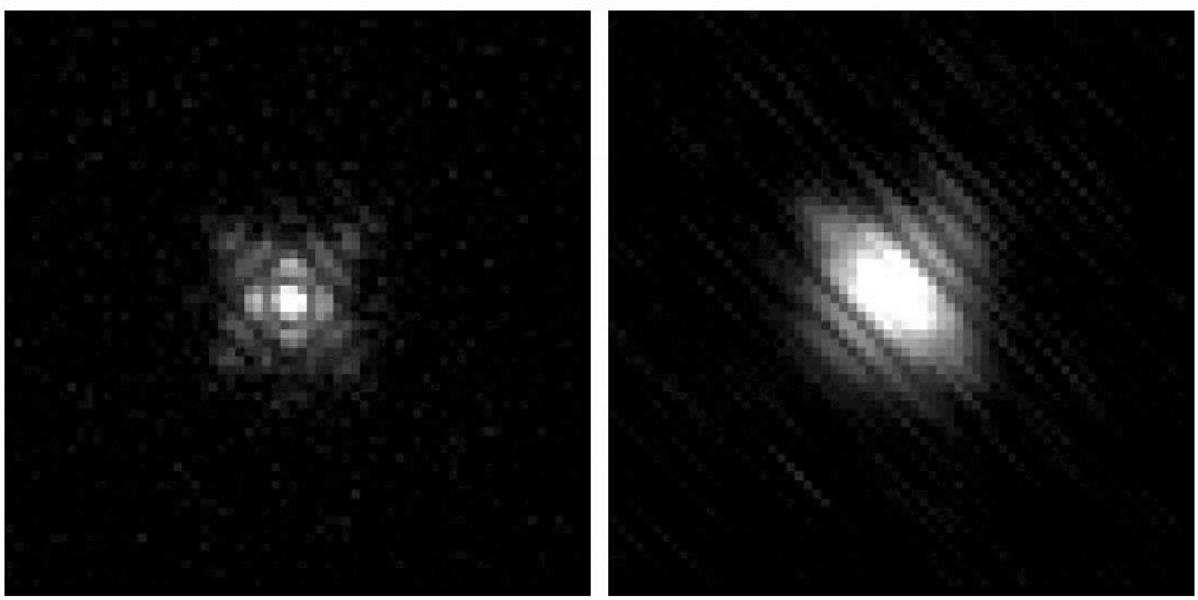

Figure 1: These two images demonstrate the effects of target drift on image quality. The image on the left represents a Palomar Adaptive Optics diffraction-limited stellar PSF taken with the PHARO camera. The image on the right was created from the identical exposure, but with a

simulated 4.2-pixel (106 mas) drift.

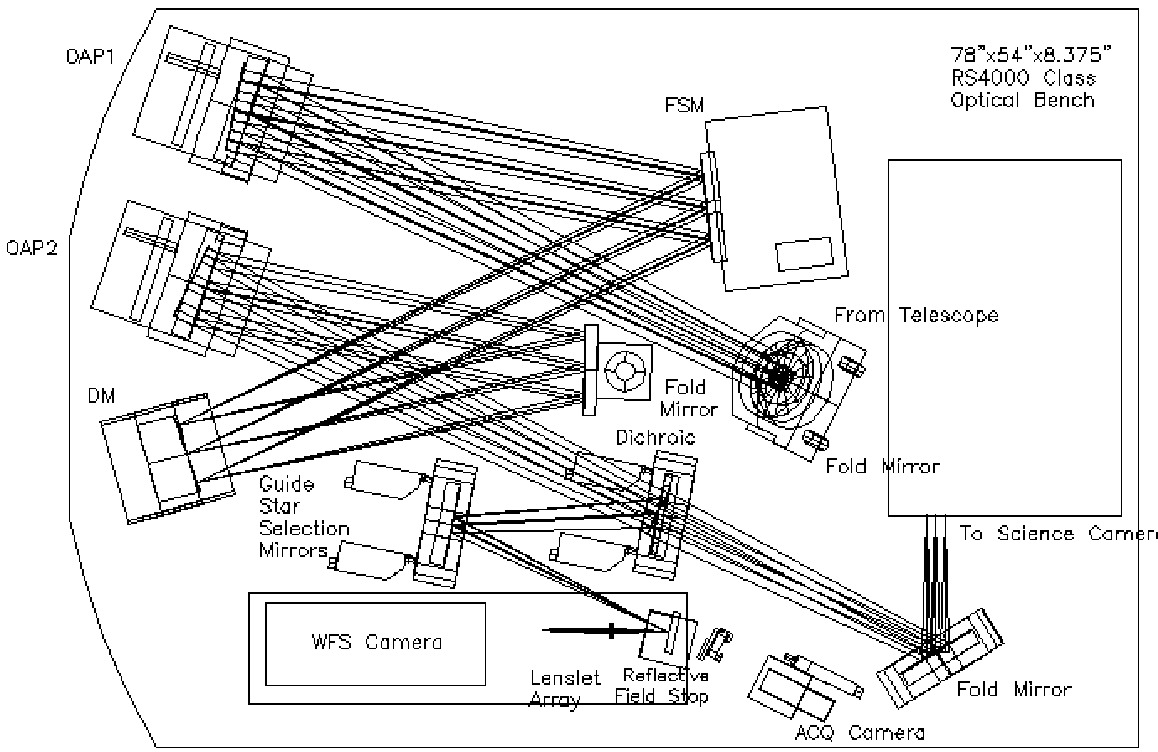

Figure 2: A schematic of the Palomar Adaptive Optics bench. The optical beam enters at the position marked “From Telescope”. The PHARO science camera is represented by the rectangle on the right side. The optic in the lower right, labeled “Fold Mirror”, has been replaced with a dichroic that allows visible light, that has leaked through the upstream dichroic, to transmit to a visible camera positioned behind the “Fold Mirror” dichroic.

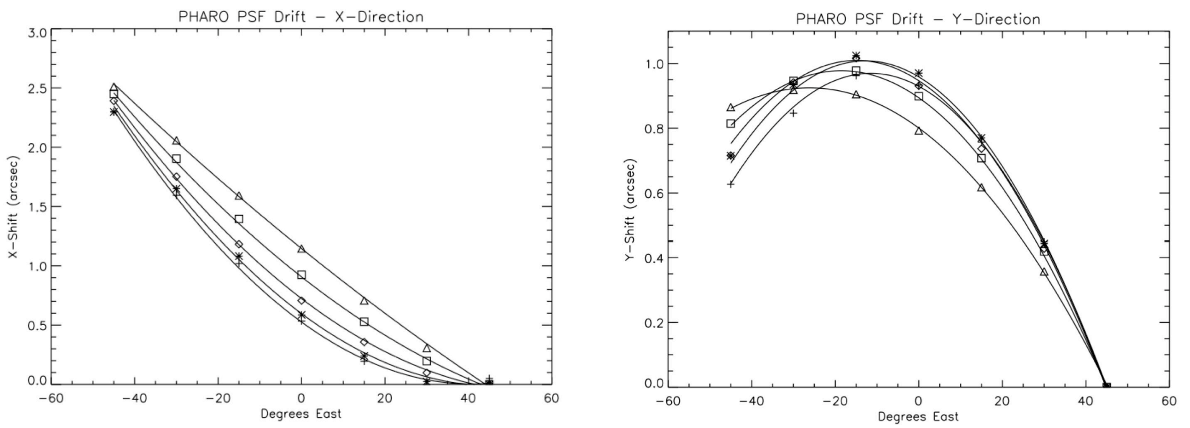

Figure 3: The above plots describe PHARO image drift as a function of hour angle, as measured in February 2006. The figure on the left represents X-direction drift and the figure on the right represents Y-direction drift. We define "drift" or "shift" as target displacement from the original target position measured at a 45-degree-east telescope position. The plotted symbols represent actual measured data. The curves represent mathematical functions described by equations 1 and 2. The data symbols correspond to the following declinations: *triangle* = 3-degree declination; *diamond* = 33-degree declination; *asterick* = 48-degree declination; *plus* = 63-degree declination; *box* = 18-degree declination. The fitted curves match the measured data with a standard error of 0.021 arcseconds (0.22%) for the x-shift and 0.008 arcseconds (0.12%) for the y-shift.

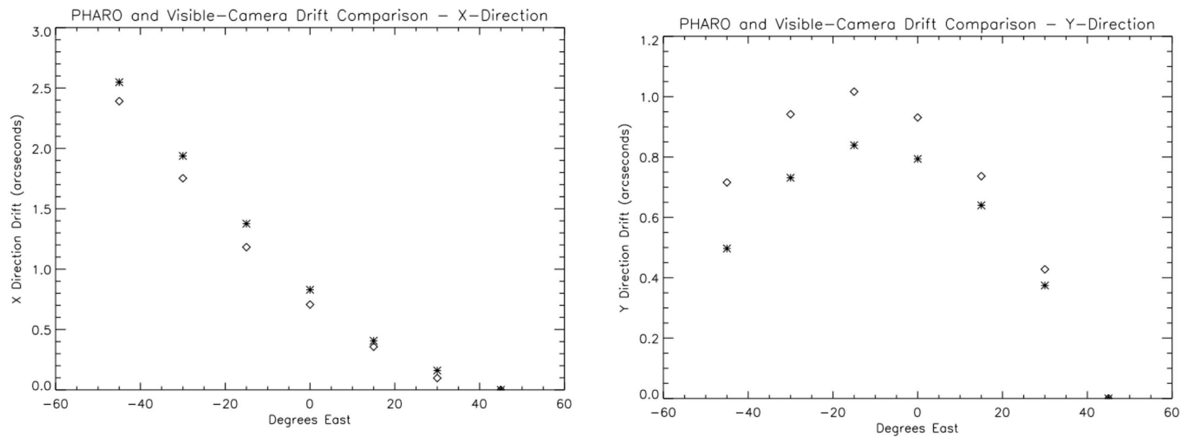

Figure 4: The plots above show a comparison of target drift, as measured simultaneously by the PHARO science camera (diamond data points) and an installed visible, flexure-monitoring camera (asterick data points). The horizontal axis represents telescope position, as measured in degrees east of zenith. The vertical axis represents image drift, in either the detector *x* or *y* dimension. "Image drift" is measured as an arcsecond displacement from the starting image position measured at a 45-degree-east telescope position. The data reveal that the flexure-monitoring camera and PHARO science camera measure drift that agree within ~15%.